Available online at www.sciencedirect.com
ScienceDirect
Bioorganic & Medicinal Chemistry 15 (2007) 4511–4519
Bioorganic & Medicinal Chemistry

Synthesis and radiopharmacological characterization of 2β-carbo-2′-[^{18}F]fluoroethoxy-3β-(4-bromo-phenyl)tropane ([^{18}F]MCL-322) as a PET radiotracer for imaging the dopamine transporter (DAT)

F. Wuest,[a,*] M. Berndt,[a] K. Strobel,[a] J. van den Hoff,[a] X. Peng,[b] J. L. Neumeyer[b] and R. Bergmann[a]

[a]*Institut für Radiopharmazie, Forschungszentrum Dresden-Rossendorf, Postfach 510119, 01314 Dresden, Germany*
[b]*McLean Hospital, Harvard Medical School, Belmont, MA 02478-9106, USA*

Received 5 October 2006; revised 5 April 2007; accepted 13 April 2007
Available online 19 April 2007

Abstract—The fluoroalkyl-containing tropane derivative 2β-carbo-2′-fluoroethoxy-3β-(4-bromo-phenyl)tropane (MCL-322) is a highly potent and moderately selective ligand for the dopamine transporter (DAT). The compound was labeled with the short-lived positron emitter ^{18}F in a single step by nucleophilic displacement of the corresponding tosylate precursor MCL-323 with no-carrier-added [^{18}F]fluoride. The positron emission tomography (PET) radiotracer 2β-carbo-2′-[^{18}F]fluoroethoxy-3β-(4-bromo-phenyl)tropane [^{18}F]MCL-322 was obtained in decay-corrected radiochemical yields of 30–40% at a specific radioactivity of 1.6–2.4 Ci/μmol (60–90 GBq/μmol) at the end-of-synthesis (EOS). Small animal PET, ex vivo and in vivo biodistribution experiments in rats demonstrated a high uptake in the striatum (3.2% ID/g) 5 min after injection, which increased to 4.2% ID/g after 60 min. The uptake in the cerebellum was 1.8% ID/g and 0.6% ID/g after 5 min and 60 min post-injection, respectively. Specific binding to DAT of [^{18}F]MCL-322 was confirmed by blocking experiments using the high affinity DAT ligand GBR 12909. The radiopharmacological characterization was completed with metabolite and autoradiographic studies confirming the selective uptake of [^{18}F]MCL-322 in the striatum. It is concluded that the simple single-step radiosynthesis of [^{18}F]MCL-322 and the promising radiopharmacological data make [^{18}F]MCL-322 an attractive candidate for the further development of a PET radiotracer potentially suitable for clinical DAT imaging in the human brain.

1. Introduction

The dopamine transporter (DAT) is a 12 α-helical membrane-bound protein that is located in the presynaptic nerve terminals and facilitates the release and reabsorption of dopamine. DAT controls the synaptic dopamine concentration in the intersynaptic cleft and thus dopamine neurotransmission in the brain. Alterations of the density and function of DAT are thought to be implicated in numerous neurodegenerative and neuropsychiatric disorders including Parkinson's disease (PD),[1,2] Alzheimer's disease (AD), major depression,[3] Huntington chorea, schizophrenia, and attention deficient-hyperactivity disorder (ADHD)[4,5] or drug abuse. The highest levels of DAT in the brain are found in striatum and olfactory tubercle, with much lower levels in amygdala, hypothalamus, hippocampus, some thalamic nuclei, and neocortex. Because the DAT density can be considered as a marker of the integrity and number of presynaptic dopamine producing neurons, which correlates with dopaminergic innervations, several specific positron-emitting DAT radioligands have been developed for imaging, monitoring, and quantitation of these neurological illnesses and disorders as well as for the evaluation of their treatment. First radiotracers for imaging of DAT in vivo by positron emission tomography (PET) included [*N*-^{11}C-methyl]cocaine[6] and its analogs such as 2β-[^{11}C]carbomethoxy-3β-(4-iodophenyl)tropane [^{11}C]β -CIT,[7] [^{11}C]2β-carbomethoxy-3β-(4-chlorophenyl)tropane ([^{11}C]CCT),[8] [^{11}C]2β-carbomethoxy-3β-

Keywords: [^{18}F]MCL-322; Dopamine transporter (DAT); Positron emission tomography (PET).
* Corresponding author. Tel.: +49 351 260 2760; fax: +49 351 260 2915; e-mail: f.wuest@fz-rossendorf.de

0968-0896/$ - see front matter © 2007 Elsevier Ltd. All rights reserved.
doi:10.1016/j.bmc.2007.04.019

(4-fluorophenyl)tropane ([^{11}C]β-CFT),[8] methyl-(1*R*-2-exo-3-exo)-8-methyl-3-(4-methylphenyl)-8-azabicyclo[3.2.1] octane-2-carboxylate ([^{11}C]RTI-32),[9] (*E*)-*N*-(4-fluoro-but-2-enyl)-[^{11}C]2β-carbomethoxy-3β-(4′-tolyl)nortropane ([^{11}C]LBT-999)[10], and, more recently, *N*-(3-iodoprop-2E-enyl)-2β-carbomethoxy-3β-(4-methylphenyl) nortropane ([^{11}C]PE2I).[11] However, some of these tropane-based ligands also display high binding to the serotonin transporter (SERT)[12] and, to a lower extent, to the norepinephrine transporter (NET). Moreover, the short half-life of ^{11}C may limit the time period of a PET scan to reach the DAT binding equilibrium.

The longer half-life of ^{18}F offers significant advantages with regard to radiosynthesis and reaching the equilibrium within the PET scan time period. Thus, several cocaine analogs labeled with ^{18}F as DAT ligands have been developed during the last decade. Some selected examples include 2β-carbo-2′-[^{18}F]fluoroethoxy-3β-(4-iodophenyl)tropane ([^{18}F]FE-CIT),[13] *N*-3-[^{18}F]fluoropropyl-2β-carbomethoxy-3β-(4-iodophenyl)nortropane ([^{18}F]FP-CIT),[14,15] 2β-carbo-2′-[^{18}F]fluoroethoxy-3β-(4-chlorophenyl)tropane ([^{18}F]FECT),[9] 2β-carbo-2′-[^{18}F] fluoroethoxy-3β-(4-methylphenyl)tropane ([^{18}F]FETT),[9] *N*-3-[^{18}F]fluoropropyl-2β-carbomethoxy-3β-(4-chlorophenyl)tropane ([^{18}F]FPCT),[16] *N*-3-[^{18}F]fluoropropyl-2β-carbomethoxy-3β-(4-methylphenyl)tropane ([^{18}F]FPCMT)[17], *N*-2-[^{18}F]fluoroethyl-2β-carbomethoxy-3β-(4-chlorophenyl)tropane ([^{18}F]FECNT),[18] *N*-2-[^{18}F]fluoroethyl-2β-carbomethoxy-3β-(4-fluorophenyl)tropane ([^{18}F]FE-CFT)[19], and *N*-(3-[^{18}F]fluoropropyl)-2β-carbomethoxy-3β-(4-bromo-phenyl)tropane ([^{18}F]FPCBT)[20] (Fig. 1).

Most of the compounds were synthesized via laborious two-step synthesis sequences involving a *N*- or *O*-[^{18}F]fluoroalkylation reaction as the key step. All these approaches made use of various [^{18}F]fluoroalkylhalides or -sulfonates as alkylating agents. A reported single step synthesis of [^{18}F]FP-CIT through nucleophilic radiofluorination using a mesylate precursor gave only very low radiochemical yields of 1–2%.[15] Although some of the ligands show promise as clinical PET imaging agents for the DAT, their affinity and selectivity profile for the DAT still require improvement. Moreover, a simpler one-step synthesis procedure is desirable to facilitate automation of the radiosynthesis.

Recently, the fluoroethyl ester-containing phenyltropane derivative 2β-carbo-2′-fluoroethoxy-3β-(4-bromophenyl)tropane (MCL-322) was shown to display high affinity to the dopamine transporter (DAT) (K_i = 2.3 nM).[21] The binding affinities (K_i values) for the serotonin transporter (SERT) and norepinephrine transporter (NET) were determined to be 5.1 and 280 nM, respectively.[21] The radioreceptor assays were carried out from striatal homogenates obtained from brain tissue from young adult male Sprague–Dawley rats by the procedure previously described by Kula and co-workers.[22] This should make the corresponding ^{18}F-labeled compound a potential PET radioligand for imaging the DAT. Here, we report the simple single step radiosynthesis of 2β-carbo-2′-[^{18}F]fluoroethoxy-3β-(4-bromophenyl)tropane ([^{18}F]MCL-322) and the radiopharmacological characterization of [^{18}F]MCL-322 in rats including biodistribution, autoradiography, and small animal PET studies without and with blocking of the DAT.

2. Results

2.1. Radiochemistry

The labeling of [^{18}F]MCL-322 was performed in a remotely controlled synthesis module via a single step radiosynthesis by treatment of the corresponding tosylate precursor MCL-323[21] with no-carrier-added potassium [^{18}F]fluoride and kryptofix K_{222} in acetonitrile at 80 °C (Fig. 2).

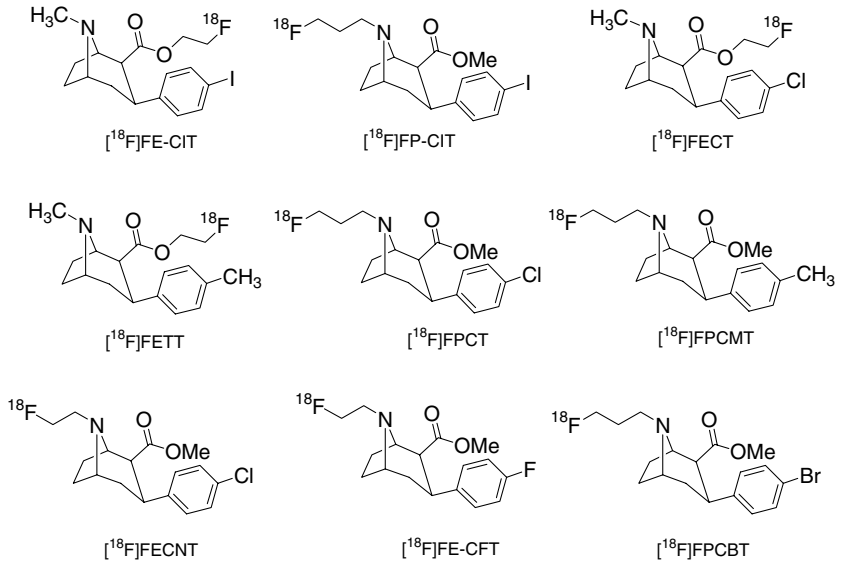

Figure 1. Selection of ^{18}F-labeled cocaine analogs as DAT ligands.

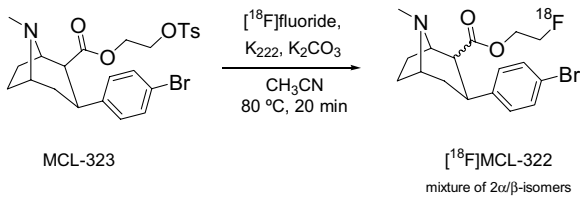

Figure 2. Radiosynthesis of [^{18}F]MCL-322.

[^{18}F]Fluoride incorporation by nucleophilic displacement of the tosylate leaving group in MCL-323 gave [^{18}F]MCL-322 in radiochemical yields of 30–40% (n = 15, decay-corrected) within 60 min including HPLC separation. Starting from 100 to 240 mCi (3.7–9 GBq) of [^{18}F]fluoride, 19–38 mCi (700–1400 MBq) of [^{18}F]MCL-322 could be prepared. The radiochemical purity exceeded 95%, and the specific radioactivity was determined to be 1.6–2.4 Ci/μmol (60–90 GBq/μmol) at the end-of-synthesis.

2.2. [^{18}F]MCL-322 biodistribution in peripheral organs

The distribution of radioactivity in selected peripheral tissues and organs, and the regional radioactivity distribution in rat brain at 5, 20, 60, 120, and 240 min after injection of [^{18}F]MCL-322 are shown in Tables 1 and 2, respectively.

The specificity and selectivity of regional brain binding of [^{18}F]MCL-322 for the dopamine transporter was studied through a series of blocking studies using known monoamine transporter specific ligands (2 mg/kg body weight of rat, intravenously) which were administered 10 min prior to injection of the radiotracer. The rats were sacrificed 60 min after radiotracer injection, and striatum, cortex, cerebellum, and hippocampus were dissected and the radioactivity concentration determined. The results are summarized in Table 3.

2.3. Ex vivo autoradiography in rat brain

The distribution of [^{18}F]MCL-322 in rat brain was further studied by ex vivo autoradiography. The visible high uptake of radioactivity in the striatum compared to the other brain regions confirms high binding of [^{18}F]MCL-322 to DAT. The radioactivity distribution in a rat brain slice at 60 min pi along with the corresponding histological section is given in Figure 3.

2.4. [^{18}F]MCL-322 metabolites

Metabolite analysis with radio-HPLC indicated that compound [^{18}F]MCL-322 was rapidly metabolized to a single polar metabolite in rat plasma. The amount of the polar metabolite steadily increased over time reaching 21% at 1.5 min, 42% at 5 min, 61% at 10 min, 76% at 30 min, 85% at 60 min, and >98% at 240 min. Metabolite analysis of supernatants of rat striatal homogenates detected predominately intact parent compound [^{18}F]MCL-322 at 60 min pi (>90%).

2.5. Small animal PET and MRI

Small animal PET studies in living rats were performed to compare and determine time–activity curves in the striatum and cerebellum. MicroPET® images were acquired from 0 to 120 min. The MR image was used to obtain the precise anatomical correlate of the high uptake areas detected in PET. The separate PET and MR image and the corresponding fused image are shown in Figure 4.

Time–activity curves were used to assess the kinetics of [^{18}F]MCL-322 binding in the striatum and cerebellum in the control experiment and after pretreatment with GBR12909. The distribution of radioactivity in the rat striatum and cerebellum over time is given in Figure 5 after intravenous administration of [^{18}F]MCL-322.

The curve for specific binding in the control experiment reveals fast entry of compound [^{18}F]MCL-322 into the brain and its accumulation in the striatum as the target region. The radioactivity concentration in the DAT-rich striatum steadily increased within the first 20 min. After 30 min the radioactivity accumulation reached its

Table 1. Biodistribution of [^{18}F]MCL-322 in peripheral tissues and organs of male Wistar rats (body weight 122 ± 16 g) after single intravenous application at various time points after injection (5, 20, 60, 120, and 240 min pi) represented as % ID/g, mean ± SD (5 animals per time point)

Time pi (min)	5	20	60	120	240
Blood	0.16 ± 0.02	0.07 ± 0.01	0.04 ± 0.01	0.03 ± 0.00	0.03 ± 0.00
Brown fat	1.46 ± 0.13	0.78 ± 0.11	0.39 ± 0.09	0.21 ± 0.03	0.08 ± 0.01
Hair and skin	0.47 ± 0.06	0.47 ± 0.04	0.29 ± 0.06	0.17 ± 0.02	0.08 ± 0.01
Pancreas	2.09 ± 0.52	1.23 ± 0.09	0.54 ± 0.18	0.29 ± 0.07	0.13 ± 0.03
Spleen	1.51 ± 0.21	1.41 ± 0.24	0.58 ± 0.10	0.29 ± 0.05	0.12 ± 0.05
Adrenals	3.57 ± 0.96	1.21 ± 0.21	0.58 ± 0.13	0.35 ± 0.06	0.17 ± 0.04
Kidneys	4.64 ± 1.33	3.51 ± 1.44	3.10 ± 0.87	1.84 ± 0.46	0.83 ± 0.25
Fat	0.57 ± 0.14	0.48 ± 0.09	0.27 ± 0.03	0.16 ± 0.04	0.06 ± 0.02
Muscle	0.42 ± 0.06	0.33 ± 0.05	0.16 ± 0.05	0.09 ± 0.02	0.04 ± 0.01
Heart	1.09 ± 0.37	0.48 ± 0.08	0.21 ± 0.04	0.12 ± 0.02	0.07 ± 0.02
Lung	6.53 ± 2.37	2.58 ± 0.28	1.14 ± 0.25	0.54 ± 0.07	0.27 ± 0.08
Thymus	0.89 ± 0.17	0.82 ± 0.12	0.41 ± 0.04	0.21 ± 0.05	0.08 ± 0.02
Harderian glands	1.46 ± 0.16	2.04 ± 0.23	2.37 ± 0.42	1.82 ± 0.37	0.93 ± 0.17
Liver	3.20 ± 1.10	6.80 ± 1.50	11.8 ± 2.50	15.7 ± 2.10	15.2 ± 1.30
Femur	0.59 ± 0.06	0.42 ± 0.04	0.17 ± 0.04	0.10 ± 0.02	0.07 ± 0.02
Testes	0.33 ± 0.05	0.45 ± 0.08	0.50 ± 0.10	0.39 ± 0.03	0.17 ± 0.04

Table 2. Regional distribution of the radiotracer in male Wistar rats, represented as % ID/g, mean ± SD (5 animals per time point)

Time (min)	5	20	60	120	240
Blood	0.16 ± 0.02	0.07 ± 0.01	0.04 ± 0.01	0.03 ± 0.00	0.03 ± 0.00
Striatum	3.23 ± 0.28	3.93 ± 0.67	4.17 ± 0.68	3.51 ± 0.41	2.45 ± 0.33
Cerebellum	1.77 ± 0.31	1.37 ± 0.25	0.56 ± 0.09	0.24 ± 0.05	0.09 ± 0.02
Cortex	3.19 ± 0.33	2.29 ± 0.25	1.00 ± 0.19	0.45 ± 0.09	0.14 ± 0.03
Hippocampus	2.37 ± 0.28	1.99 ± 0.28	1.12 ± 0.31	0.42 ± 0.07	0.18 ± 0.06
Rest of brain	2.53 ± 0.22	2.06 ± 0.3	1.10 ± 0.2	0.59 ± 0.08	0.27 ± 0.05
Striatum/blood	20.2 ± 4.3	56.1 ± 17.6	104 ± 43	117 ± 14	81.7 ± 11.0
Striatum/cerebellum	1.8 ± 0.5	2.9 ± 1.0	7.4 ± 2.4	14.6 ± 4.8	27.2 ± 9.7

Table 3. Biodistribution of [^{18}F]MCL-322 in male Wistar rat brains after single intravenous application (% ID/g, mean ± SD, 2 animals per group) at 60 min pi without (control) or with pre-injection of GBR12909, citalopram or nisoxetine (mean ± SD in % ID/g tissue)

	Control	GBR12909	Citalopram	Nisoxetine
Blood	0.025 ± 0.014	0.040 ± 0.020	0.052 ± 0.013	0.040 ± 0.009
Striatum	3.71 ± 0.16	1.51 ± 0.36*	6.43 ± 1.48	4.18 ± 0.14
Cortex	1.04 ± 0.32	0.94 ± 0.21	0.97 ± 0.29	0.96 ± 0.21
Cerebellum	0.67 ± 0.15	0.62 ± 0.10	0.71 ± 0.07	0.63 ± 0.06
Hippocampus	1.10 ± 0.18	1.06 ± 0.19	1.36 ± 0.01	0.91 ± 0.01
Rest of brain	1.37 ± 0.14	1.07 ± 0.18	1.56 ± 0.29	1.23 ± 0.02

*$P < 0.05$ in comparison to the cerebellum.

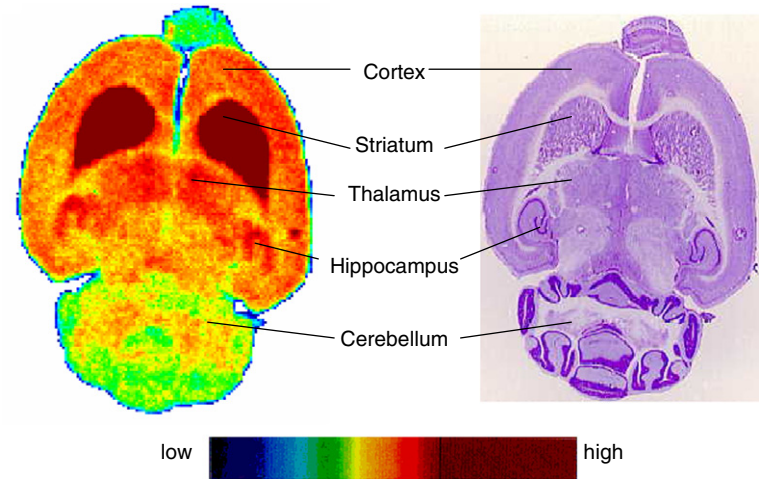

Figure 3. Autoradiogram (left) of horizontal planes of the rat brain at 60 min after injection of [^{18}F]MCL-322, radioactivity standard, and corresponding histological section (right).

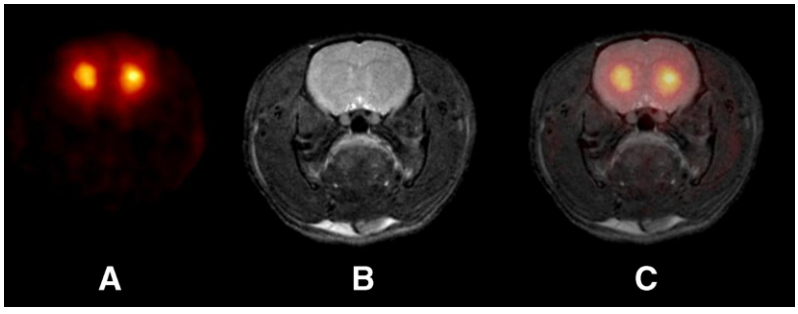

Figure 4. Transaxial images through the striatum of a Wistar rat at 60 min pi: PET image of [^{18}F]MCL-322 (A), corresponding MRT image (B), and the fused image (C).

maximum, and the radioactivity concentration in the striatum remains stable until the end of data acquisition (115 min). The radioactivity concentration in the cerebellum as the reference region increased rapidly within the first 5 min. It peaked between 7 and 8 min, and a continuous washout of radioactivity from the

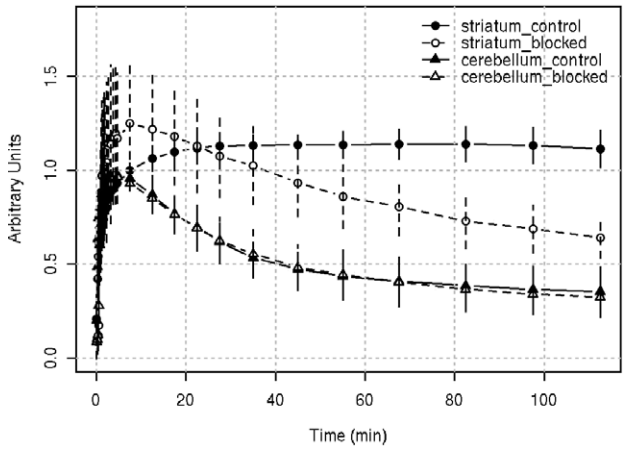

Figure 5. Time–activity curves (TACs) after injection of [^{18}F]MCL-322 in the rat brain (striatum and cerebellum). Shown are averages (±SD) of 5 control studies and 4 studies after blocking with GBR 12909 (2 mg/kg body weight, intravenously), respectively. Averages were computed after individual normalization of each study to a peak value of one for the cerebellum curve (to compensate for interindividual variations in injected dose).

cerebellum is observed until the end of the PET study. Pretreatment with GBR12909 significantly decreased the radioactivity uptake in the striatum (Fig. 5).

3. Discussion

Quantification of the dopamine terminal function by PET remains an important challenge. Over the last decade several ^{18}F-labeled cocaine analogs have been prepared that bind to dopamine transporter on nigrostriatal terminals. However, the DAT is potentially subject to compensatory regulation and direct pharmacological effects.[23,24] For discrimination of these processes, high selectivity, negligible binding to other receptors, and low metabolism in the brain seem to be central attributes of DAT radiotracers.

The synthesized ^{18}F-labeled cocaine analogs show different substitution pattern on the ester function at position 2β, the amine function and the substituent in the para position of the aromatic ring at position 3β. Most compounds were synthesized via a two-step reaction sequence involving a *N*- or *O*-alkylation with [^{18}F]fluoroalkylhalides or -sulfonates. Although moderate overall radiochemical yields of about 20% (decay-corrected) could be obtained for compound [^{18}F]FECNT,[18,25] however, most of the compounds prepared via the two-step reaction sequence gave only very low radiochemical yields of 1–5% (not corrected for decay).[15,17,20] The presented single step radiosynthesis of [^{18}F]MCL-322 via nucleophilic substitution with no-carrier-added [^{18}F]fluoride gave the radiotracer in reasonable radiochemical yields of 30–40% (decay-corrected). Thus, the radiochemical yields are much higher compared to the very low radiochemical yield (1–2%, without decay correction) obtained by the reported single step radiosynthesis of [^{18}F]FP-CIT.[15]

In the reaction mixture a more lipophilic side-product could be detected. This side-product may be due to the epimerization of the tropane ring at position 2 to form the thermodynamically more stable α-isomer rather than the desired β-isomer. The α/β epimerization of the tropane ring at position 2 is a well-known fact, which has also been reported as a drawback within the synthesis of several ^{18}F-labeled tropanes as DAT ligands.[15,20,26] However, the formed α-isomer could easily be separated through semi-preparative HPLC purification of the reaction mixture. It was found that the reaction temperature of 80 °C seems to be optimal for sufficient fluorine-18 incorporation while reducing the extent of the epimerization reaction to form the α-isomer. A lower reaction temperature of 80 °C resulted in a drastic decrease of radiochemical yield, whereas higher reaction temperatures (>80 °C) increased the rate of the epimerization reaction leading to higher amounts of the undesired α-isomer. The specific radioactivity (1.3–1.7 Ci/μmol) obtained at time of injection of 1 mCi of [^{18}F]MCL-322 corresponds to a dose of 0.22–0.28 μg of MCL-322, which should be high enough to study DAT in the rat brain.

Compound [^{18}F]MCL-322 represents a bromo-substituted analog within a series of ^{18}F-labeled DAT ligands showing a fluoroethyl ester substitution pattern at position 2β while differing from the para-substituent at the phenyl ring, being iodine for [^{18}F]FE-CIT,[13] chlorine for [^{18}F]FECT[9], and methyl for [^{18}F]FETT.[9] Based upon ACD-Lab® calculations the lipophilicity (log *P* value) of [^{18}F]MCL-322 was determined to be 3.87 which is between the determined log *P* values of analog compounds [^{18}F]FE-CIT (4.13), [^{18}F]FECT (3.70), and [^{18}F]FETT (3.56). The distribution of radioactivity after intravenous injection of [^{18}F]MCL-322 in peripheral organs and tissues in rats is comparable to that of [^{18}F]FE-CIT, [^{18}F]FECT, and [^{18}F]FETT.

The overall very low plasma level of radioactivity measured between 5 and 240 min is a consequence of the fast blood clearance of the radiotracer including. The whole-blood radioactivity remains stable (0.03% ID/g) from 60 to 240 min post-injection. High initial levels of radioactivity were found in the lungs (6.53 ± 2.37% ID/g), kidneys (4.64 ± 1.33% ID/g), adrenals (3.57 ± 0.96% ID/g), and liver (3.20 ± 1.10% ID/g) at 5 min after administration of the radiotracer. Apart from the liver, all other organs show clearance of radioactivity over time. Thus, lungs (0.27 ± 0.08% ID/g), kidneys (0.83 ± 0.25% ID/g), and adrenals (0.17 ± 0.04% ID/g) show significantly reduced radioactivity level after 240 min pi, whereas radioactivity is accumulated in the liver over time, reaching 15.2 ± 1.3% ID/g after 240 min. A comparable radioactivity accumulation in the liver has also been observed with the iodine- and chlorine-containing compounds [^{18}F]FE-CIT and [^{18}F]FECT, whereas [^{18}F]FETT showed clearance of radioactivity from the liver. This may reflect differences in the metabolism of 4-halogen-substituted and more lipophilic compounds [^{18}F]FE-CIT, [^{18}F]MCL-322, and [^{18}F]FECT, and less lipophilic methyl-substituted [^{18}F]FETT.

Intermediate uptake was found in the heart, pancreas, and spleen, whereas bone (max. 0.59% ID/g at 5 min) and muscle (max. 0.42% ID/g at 5 min) showed only little uptake. The low uptake of radioactivity in the bone (0.10% ID/g at 120 min) after injection of [^{18}F]MCL-322 indicates that in vivo radiodefluorination is a minor metabolic process as it is the case for [^{18}F]FE-CIT (0.10% ID/g at 120 min), [^{18}F]FECT (0.11% ID/g at 120 min), and [^{18}F]FETT (0.07% ID/g at 120 min).

The observed regional distribution of radioactivity after intravenous injection of [^{18}F]MCL-322 in the rat brain agrees with that of other DAT selective radiotracers[9,17,26] and corresponds well to the known distribution of DAT in the rat brain.[9] The high accumulation of radioactivity in the brain is indicative of an efficient blood–brain-barrier passage of compound [^{18}F]MCL-322. After 5 min pi the highest regional brain uptake is found in the striatum (3.23 ± 0.28% ID/g). The radioactivity accumulation peaked in the striatum at 60 min (4.17 ± 0.68% ID/g) after radiotracer application. The radioactivity level in the striatum remained relatively stable between 20 min (3.93 ± 0.67% ID/g) and 120 min (3.51 ± 0.41% ID/g) followed by a slow wash-out reaching 2.45 ± 0.33% ID/g at 240 min. Cortex (3.19 ± 0.33% ID/g) and the hippocampus (2.37 ± 0.28% ID/g) displayed high initial radioactivity uptake at 5 min which continuously decreased to the level of the radioactivity concentration in the cerebellum (0.09 ± 0.02 % ID/g) at 240 min. Cortex, hippocampus, and cerebellum show comparable rapid washout rates of radioactivity. The regional biodistribution of radioactivity in the rat brain shows an increasing striatum/cerebellum ratio over time, being 1.8 ± 0.5 at 5 min, 2.9 ± 1.0 at 20 min, 7.4 ± 2.4 at 60 min, 14.6 ± 4.8 at 120 min, and 27.2 ± 9.7 at 240 min, respectively. The striatum/blood ratio (117 ± 14) peaked at 120 min. The measured striatum/cerebellum ratios of 1.8 at 5 min, 7.4 at 60 min, and 14.6 at 120 min agree with the data observed for [^{18}F]FECT (1.8 at 5 min, 6.9 at 60 min, and 14.0 at 120 min) and [^{18}F]FETT (1.75 at 5 min, 10.4 at 60 min, and 21.0 at 120 min). The smaller striatum/cerebellum ratios found for [^{18}F]FE-CIT (1.5 at 5 min, 3.7 at 60 min, and 3.0 at 120 min) seem to indicate a faster washout of radioactivity from the striatum. This observation is somewhat surprising since cold FE-CIT exhibited excellent in vitro affinity toward the DAT (K_i = 0.9 nM) and moderate selectivity for DAT over SERT and NET.[21] Thus, these data make [^{18}F]MCL-322 (log P = 3.87) more comparable with the slightly less lipophilic chlorine-containing [^{18}F]FECT (log P = 3.7) rather than to the more lipophilic iodine-containing [^{18}F]FE-CIT (log P = 4.13).

The data obtained within the blocking studies clearly demonstrate that administration of the dopamine transporter ligand GBR12909[27] significantly reduced uptake of the radiotracer in the striatum (1.51 ± 0.36% ID/g) compared to controls (3.71 ± 0.16% ID/g). This finding suggests that binding of [^{18}F]MCL-322 in this brain region is associated with the dopamine reuptake site. Pretreatment with citalopram and nisoxetine, which bind to the serotonin transporter (SERT) and norepinephrine transporter (NET), respectively, did not reduce the radiotracer uptake in the striatum confirming the selective binding of [^{18}F]MCL-322 to DAT. Instead of a reduction of radiotracer uptake, pre-injection of citalopram and nisoxetine increased the radioactivity level in the striatum to 6.43 ± 1.48% ID/g and 4.18 ± 0.14% ID/g, respectively. Although the reason for this observed increase remains unclear, similar effects have been reported in the literature when in vivo blocking studies of DAT with SERT and NET specific blockers were performed.[9,28]

The autoradiography (Fig. 3) of an ex vivo horizontal brain slice shows that [^{18}F]MCL-322 binds with high intensity in the rat striatum. Lower uptake is found in regions rich in serotonin uptake sites such as thalamus and cortex. Very low accumulation could be seen in the cerebellum, a region almost devoid of DAT.[29] This observed distribution pattern is consistent with DAT distribution in the rat brain reported in the literature,[30–32] and confirms the reported binding potency of MCL-322 to the serotonin transporter (K_i = 5.1 nM) and the in vitro DAT/SERT selectivity of 2.2 for MCL-322.[21]

A rapid metabolism of [^{18}F]MCL-322 in rat blood resulted in the formation of a single polar metabolite. The amount of original [^{18}F]MCL-322 in the blood decreased from 79% at 2 min pi to 58% at 5 min, 39% at 10 min, and 5% at 60 min, respectively. In contrast to the fast metabolism of [^{18}F]MCL-322 in rat blood, metabolite analysis in the striatum detected more than 90% of the intact parent compound beside a more polar compound at 60 min pi. All these data indicate that no lipophilic metabolites, which potentially could pass the blood–brain-barrier, were formed, and only minor amounts of polar metabolites could have penetrated through the blood–brain-barrier. Thus, the absence of interfering metabolites that may confound subsequent PET imaging studies is an important prerequisite to further consider [^{18}F]MCL-322 as a potential PET ligand for imaging DAT. Moreover, 84% of intact [^{18}F]MCL-322 was found in the liver as an organ of peripheral metabolism at 60 min p.i.. This surprisingly high amount of unmetabolized [^{18}F]MCL-322 in the liver agrees with the reported higher metabolic stability of alkylesters when a fluoroalkyl-chain is used.[13]

The dominant accumulation of radioactivity in the rat striatum as seen in the small animal PET studies, whilst showing only low uptake in the cerebellum, further confirms [^{18}F]MCL-322 as a suitable ligand for PET imaging of DAT. Within the time frame of the PET study (0–120 min) the general course of the time–activity curves agrees with the data obtained for the ex vivo regional biodistribution study of the radiotracer (Table 2). The maximum of radioactivity uptake in the striatum is reached at 25 min, and radioactivity level remains relatively stable between 25 and 100 min. Thereafter, a slight washout is observed. The striatum-to-cerebellum ratio was 1.5 after 20 min, 2.5 after 60 min, and 2.8 after 115 min. The uptake in the striatum could significantly be reduced by the pretreatment with GBR12909. In comparison to the control a reduction of radioactivity

uptake to 67% at 20 min, 41% at 60 min, and 36% at 115 min could be observed. These data agree very well with the observed 40% reduction of radioactivity uptake at 60 min when GBR12909 was used to inhibit [^{18}F]MCL-322 uptake in the biodistribution study (Table 3). The comparable course of the time–activity curves in the cerebellum for the control and blocking studies confirms the cerebellum as suitable reference region (Fig. 5). In the blocking studies the striatum-to-cerebellum ratio reaches 1.8 after 60 min which remains stable until the end of the measurement (115 min). However, as it can be seen in Figure 5, equilibrium is not reached in the blocked striatum within the available time window. While this behavior prevents the direct estimation of the volume of distribution (or B_{max}) from the late-time equilibrium ratio, it is still possible to derive the parameters of interest by tracer-kinetic modeling using the cerebellum as a reference region.

4. Conclusion

The selective accumulation of [^{18}F]FMCL-322 in rat brain regions of high DAT density, the absense of interfering metabolites, and the convenient and reliable single-step radiosynthesis providing reasonable radiochemical yields are important prerequisites to make this radiotracer a potentially promising candidate for DAT imaging in the human brain. However, the compound still has to be characterized in non-human primates to verify the results obtained in this paper for rats prior to its application in humans. Further studies are under way to clarify the situation whether the compound is a good candidate to study DAT in humans.

5. Materials and methods

5.1. Radiochemistry

The tosylate precursor MCL-323 and the reference compound MCL-322 were synthesized according to literature procedures.[21] MCL-323, tosylate precursor as well as cold MCL-322 were fully characterized by elemental analysis (C,H,N), mass spectrometry, and proton NMR spectroscopy as reported in[21] (compounds **17** and **18** in Table 1, respectively). The purity of [^{18}F]MCL-322 was established by comparison with authentic sample of cols MCL-322 by HLC analysis.

[^{18}F]Fluoride was produced by the ^{18}O(p,n) ^{18}F nuclear reaction on an enriched water target using an IBA CYCLONE 18/9 cyclotron. Radiosynthesis was carried out in a commercially available synthesis module for nucleophilic radiofluorination (GE Medical Systems, Muenster, Germany). The synthesis module was modified with regard to software as well as hardware. HPLC analyses were performed on a LaChrom HPLC-system from Merck-Hitachi. The chemical and radiochemical purity was determined with a Phenomenex RP18 column (125 × 3 mm, 5 μm) isocratically eluted with acetonitrile/water (80/20) containing 0.2% triethylamine at a flow rate of 1.0 ml/min.

Semipreparative HPLC purification was carried out with a Nucleosil C18 column isocratically eluted with acetonitrile/water (80/20) containing 0.2% triethylamine at a flow rate of 3 ml/min from 0 to 8 min, and at a flow rate of 5 ml/min from 8 to 20 min.

5.1.1. Preparation of 2β-carbo-2′-[^{18}F]fluoroethoxy-3β-(4-bromophenyl)tropane ([^{18}F]MCL-322). The module-assisted one-pot synthesis of [^{18}F]MCL-322 commenced with elution of [^{18}F]fluoride (100–240 mCi; 3.7–9.0 GBq) from the anion exchange cartridge into the reaction vessel using a solution of Kryptofix 2.2.2 (15 mg; 40 μmol) and potassium carbonate (2.77 mg; 20 μmol) in aqueous acetonitrile (1.5 ml; 66% acetonitrile). The solvent was evaporated by means of a vacuum and a nitrogen stream at 90 °C. The reaction mixture was carefully dried by addition and evaporation of anhydrous acetonitrile (3 ml). To the dried residue tosylate precursor MCL-323 (4.0 mg, 7.65 μmol) in acetonitrile (1.0 ml) was added and the mixture was heated at 80 °C for 20 min. HPLC eluent (2 ml) was added before injection of the reaction mixture onto the semi-preparative HPLC column. Compound [^{18}F]MCL-322 was eluted after 10–11 min. The separated fraction of [^{18}F]MCL-322 was collected in the mixing vessel containing water (25 ml). The water-diluted solution was passed through the reversed phase C18 cartridge (LiChrolut RP-18) for solid phase extraction. After washing the cartridge with water (5 ml), [^{18}F]MCL-322 was eluted with ethanol (1 ml) into the product vial containing 9 ml of saline (0.9%). HPLC-analysis: CH_3CN/0.2% TEA (80/20), t_R = 6.5 min.

5.2. Biodistribution studies in rats

All animal experiments were carried out in compliance with the German law relating to conduct of animal experimentation and approved by the regional council for animal care. The Wistar rats were housed under standard conditions with free access to standard food and tap water. Five animals (body weight 122 ± 16 g) for each time point were intravenously injected with approximately 300 μCi (11 MBq) [^{18}F]MCL-322 in 0.5 ml saline with 10% ethanol. Animals were euthanized at 5, 20, 60, 120, and 240 min post-injection. Blood, frontal cortex, cerebellum, striatum, hippocampus, and the major organs were collected, weighed, and counted in a Packard Cobra II gamma counter. The activity in the selected tissues and organs was expressed as percent injected dose per gram tissue (% ID/g). The activity of the tissue samples was decay-corrected and calibrated by comparing the counts in tissue with the counts in aliquots of the injected tracer that had been measured in the gamma counter at the same time. Values are quoted as means ± standard deviation (mean ± SD) for a group of five animals.

In blocking experiments DAT ligand GBR12909, SERT ligand citalopram or NET ligand nisoxetine (2 mg/kg body weight each) was injected intravenously 10 min prior to tracer application. In the corresponding control group the rats were injected with saline. The animals in each group were sacrificed 60 min after the injection of the radiotracer. The average % ID/g in the control group

was compared with the groups pretreated with GBR12909, citalopram, and nisoxetine.

5.3. Ex vivo autoradiography

Male Wistar rats (body weight 100 ± 6 g) were intravenously injected with approximately 1 mCi (37 MBq) of [^{18}F]MCL-322 in a volume of 0.5 ml saline with 10% ethanol. The specific activity of the injected radiotracer was 1.3–1.7 Ci/μmol (48–63 GBq/μmol) at the time of injection. The animals were sacrificed by CO_2 inhalation at 60 min after the radiotracer injection. The brains were removed and quickly frozen by immersion in isopentane/dry ice solution at −50 °C. The frozen brains were weighed and the activity concentration was determined in a γ-well counter (Isomed 2000, Germany). The stage-mounted brains were cut on a cryostat microtome (CM 1850, Leica Instruments, Germany) into 20 μm horizontal sections, which were thaw-mounted onto microscope slides (Super Frost, Menzel, Germany), dried under a continuous cold air stream, and exposed to imaging plates (BAS-SR Imaging Plate, FUJI, Japan) together with a tissue activity standard overnight. The imaging plates were scanned in the bio-imaging analyzer BAS 5000 (FUJI, Japan). The data were recorded as photostimulated luminescence values (PSL), which are proportional to the radioactivity of the measured sample. The data analysis was carried out with the software program AIDA (Raytest, Germany). After exposure, the brain sections were stained with cresyl violet to match anatomical with functional information.

5.4. Metabolite analysis

[^{18}F]MCL-322 (37 MBq, 1 mCi) was injected intravenously into male Wistar rats under isoflurane (1.5%) oxygen anesthesia. Blood samples from the arteria femoralis dexter were taken using a catheter at 1.5, 5, 10, 30, and 60 min after injection. Plasma was separated by centrifugation (3 min, 11,000*g*), followed by precipitation of the plasma proteins with ice-cold methanol (1.5 parts per 1 part plasma) and centrifugation (3 min, 11,000*g*), and the supernatants were analyzed by HPLC. At 60 min after injection, the brains were immediately removed and the striatum was dissected. The tissues were homogenized (10% w/v in isotonic sodium chloride, at 4 °C), the homogenates were centrifuged (3 min, 11,000*g*), and the supernatants were treated as the plasma samples to receive protein-free extracts, which were analyzed by radio-HPLC. The radio-HPLC system (Agilent 1100 series) applied for metabolite analysis was equipped with UV detection (210 nm) and an external radiochemical detector (Canberra-Packard, Radiomatic Flo-one Beta 150TR) with PET flow cell. Analysis was performed on a Zorbax SP IV (250 × 9.4 mm, 7 μm) with a methanol/phosphate buffer (0.01 M, pH 7.4) gradient with 2 ml/min.

5.5. PET imaging

General anesthesia of rats was induced with inhalation of 3% isoflurane in oxygen, and was maintained with 1.5% isoflurane in oxygen and subsequently fixed in prone position on the microPET® bed. In the PET experiments, 1 ± 0.2 mCi (37 ± 7 MBq) of [^{18}F]MCL-322 in 0.5 ml saline was administered intravenously as a bolus via a tail vein. In the blocking experiments the DAT ligand GBR12909 (2 mg/kg body weight) was injected intravenously 10 min prior to radiotracer application.

PET imaging of [^{18}F]MCL-322 in rat brain was performed over 120 min with a microPET® P4 scanner, (Siemens CTI Molecular Imaging Inc. Knoxville). Data acquisition was performed in 3D list mode. A transmission scan was carried out prior to the injection of [^{18}F]MCL-322 using a ^{137}Cs point source. Emission data were collected continuously for 120 min after injection of [^{18}F]MCL-322. The list mode data were sorted into 4 sinograms for the 30 min frames and for the dynamic study using a framing scheme of 12 × 10 s, 6 × 30 s, 5 × 300 s, 9 × 600 s frames. The data were attenuation corrected and the static 30 min frames (30–60 min pi) were reconstructed by filtered back projection using a ramp filter. The pixel size was 0.949 by 0.949 by 1.212 mm and the resolution was around 1.85 mm. No correction for recovery and partial volume effects was applied. The image files were processed using the ASIPro software (Siemens, CTI Concorde Microsystems Inc. Knoxville) and the ROVER software (ABX medical software development, Radeberg, Germany). A summed image from 30 to 60 min pi was used to define the regions of interest (ROI). The data were normalized to the injected radioactivity by using ^{18}F standards from the injection solution measured in a γ-well counter (Isomed 2000, Germany), cross-calibrated to the PET scanner, and expressed in percent of injected dose per cubic centimeter (% ID/cm^3).

5.6. microMRT imaging

The MR images were acquired with a 7 T small animal scanner (BioSpec 70/30, Bruker BioSpin MRI GmbH, Ettlingen, Germany) equipped with a mini imaging gradient coil system (gradient strength 400 mT/m) and a 1H transmit-receive quadrature coil with 72 mm inner diameter.

Images were acquired using a 3D slab-selective turboRARE sequence (repetition time = 1200 ms, echo time = 42.9 ms, RARE partitions = 16) with matrix size ($X \times Y \times Z$) of 256 × 256 × 40 and a field of view of (40 × 40 × 40) mm. Image fusion of the PET and MR images was performed using the Multi Purpose Imaging Tool (MPI Tool, ATV GmbH, Germany).

5.7. Statistical analysis

The data are expressed as means ± SD. One-way analysis of variance (ANOVA) was used for statistical evaluation. Means were compared using Student's *t* test. A P value of <0.05 was considered significant and indicated by an asterisk symbol (*).

Acknowledgments

The authors would like to thank Marion Kretzschmar, Beate Pawelke, Heidemarie Kasper, Regina Herrlich,

and Stephan Preusche for their excellent technical assistance. The studies at Harvard Medical School (McLean Hospital) were supported by a grant from the National Institute of Neurological Disorders and Stroke (NS-40587, to J. L. N.).

References and notes

1. Niznik, H. B.; Fogel, E. F.; Fassos, F. F.; Seeman, P. *J. Neurochem.* **1991**, *56*, 192–198.
2. Rinne, J. O.; Bergman, J.; Ruottinen, H.; Haaparanta, M.; Eronen, E.; Oikonen, V.; Sonninen, P.; Solin, O. *Synapse* **1999**, *31*, 119–124.
3. Kapur, S.; Mann, J. J. *Biol. Psychiatry* **1992**, *32*, 1–17.
4. Dougherty, D. D.; Bonab, A. A.; Spencer, T. J.; Rauch, S. L.; Madras, B. K.; Fischman, A. J. *Lancet* **1999**, *354*, 2132–2133.
5. Dresel, S.; Krause, J.; Krause, K. H.; LaFougere, C.; Brinkbaumer, K.; Kung, H. F.; Hahn, K.; Tatsch, K. *Eur. J. Nucl. Med.* **2000**, *27*, 1518–1524.
6. Fowler, J. S.; Volkow, N. D.; Wolf, A. P.; Dewey, S. L.; Schlyer, D. J.; Macgregor, R. R.; Hitzemann, R.; Logan, J.; Bendriem, B.; Gatley, S. J., et al. *Synapse* **1989**, *4*, 371–377.
7. Müller, L.; Halldin, C.; Farde, L.; Karlsson, P.; Hall, H.; Swahn, C. G.; Neumeyer, J.; Gao, Y.; Milius, R. *Nucl. Med. Biol.* **1993**, *20*, 249–255.
8. Wong, D. F.; Yung, B.; Dannals, R. F.; Shaya, E. K.; Ravert, H. T.; Chen, C. A.; Chan, B.; Folio, T.; Scheffel, U.; Ricuaurte, G. A.; Neumeyer, J. L.; Wagner, H. N.; Kuhnar, M. J. *Synapse* **1993**, *15*, 185–191.
9. Wilson, A. A.; DaSilva, J. N.; Houle, S. *Nucl. Med. Biol.* **1996**, *23*, 141–146.
10. Dolle, F.; Emond, P.; Mavel, S.; Demphel, S.; Hinnen, F.; Mincheva, Z.; Saba, W.; Valette, H.; Chalon, S.; Halldin, C.; Helfenbein, J.; Legaillard, J.; Madelmont, J. C.; Deloye, J. B.; Bottlaender, M.; Guilloteau, D. *Bioorg. Med. Chem.* **2006**, *14*, 1115–1125.
11. Jucaite, A.; Odano, I.; Olsson, H.; Pauli, S.; Halldin, C.; Farde, L. *Eur. J. Nucl. Med. Mol. Imaging* **2006**, *33*, 657–668.
12. Bois, F.; Baldwin, R. M.; Kula, N. S.; Baldessarini, R. J.; Al Tikriti, M.; Innis, R. B.; Tamagnan, G. D. *Bioorg. Med. Chem.* **2006**, *16*, 5222–5225.
13. Mitterhauser, M.; Wadsak, W.; Mien, L. K.; Hoepping, A.; Viernstein, H.; Dudczac, R.; Kletter, K. *Synapse* **2005**, *55*, 73–79.
14. Kazumata, K.; Dhawan, V.; Chaly, T.; Antonini, A.; Margouleff, C.; Belakhlef, A.; Neumeyer, J.; Eidelberg, D. *J. Nucl. Med.* **1998**, *39*, 1521–1530.
15. Chaly, T.; Dhawan, V.; Kazumata, K.; Antonini, A.; Margouleff, C.; Dahl, J. R.; Belakhlef, A.; Margouleff, D.; Yee, A.; Wang, S.; Tamagnan, G.; Neumeyer, J. L.; Eidelberg, D. *Nucl. Med. Biol.* **1996**, *23*, 999–1004.
16. Goodman, M. M.; Keil, R.; Shoup, T. M.; Eshima, D.; Eshima, L.; Kilts, C.; Votaw, J.; Camp, V. M.; Votaw, D.; Smith, E.; Kung, M. P.; Malveaux, E.; Watts, R.; Huerkamp, M.; Wu, D.; Garcia, E.; Hoffman, J. M. *J. Nucl. Med.* **1997**, *38*, 119–126.
17. Chaly, T., Jr.; Matacchieri, R.; Dahl, R.; Dhawan, V.; Eidelberg, D. *Appl. Radiat. Isot.* **1999**, *51*, 299–305.
18. Goodman, M. M.; Kilts, C. D.; Keil, R.; Shi, B.; Martarello, L.; Xing, D.; Votaw, J.; Ely, T. D.; Lambert, P.; Owens, M. J.; Camp, V. M.; Malveaux, E.; Hoffman, J. M. *Nucl. Med. Biol.* **2000**, *27*, 1–12.
19. Harada, N.; Ohba, H.; Fukumoto, D.; Kakiuchi, T.; Tsukada, H. *Synapse* **2004**, *54*, 37–45.
20. Chaly, T.; Baldwin, R. M.; Neumeyer, J. L.; Hellman, M. J.; Dhawan, V.; Garg, P. K.; Tamagnan, G.; Staley, J. K.; Al-Tikriti, M. S.; Hou, Y.; Zoghbi, S. S.; Gu, X. H.; Zong, R.; Eidelberg, D. *Nucl. Med. Biol.* **2004**, *31*, 125–131.
21. Peng, X.; Zhang, A.; Kula, N. S.; Baldessarini, R. J.; Neumeyer, J. L. *Bioorg. Med. Chem. Lett.* **2004**, *14*, 5635–5639.
22. Kula, N. S.; Baldessarini, R. J.; Tarazi, F. I.; Fisser, R.; Wang, S.; Trometer, J.; Neumeyer, J. L. *Eur. J. Pharmacol.* **1999**, *385*, 291–294.
23. Brooks, D. J. *NeuroRx* **2004**, *1*, 482–491.
24. Brooks, D. J. *NeuroRx* **2004**, *1*, 243–254.
25. Davis, M. R.; Votaw, J. R.; Bremner, J. D.; Byas-Smith, M. G.; Faber, T. L.; Voll, R. J.; Hoffman, J. M.; Grafton, S. T.; Kilts, C. D.; Goodman, M. M. *J. Nucl. Med.* **2003**, *44*, 855–861.
26. Xing, D.; Chen, P.; Keil, R.; Kilts, C. D.; Shi, B.; Camp, V. M.; Malveaux, G.; Ely, T.; Owens, M. J.; Votaw, J.; Davis, M.; Hoffman, J. M.; BaKay, R. A.; Subramanian, T.; Watts, R. L.; Goodman, M. M. *J. Med. Chem.* **2000**, *43*, 639–648.
27. Heikkila, R. E.; Manzino, L. *Eur. J. Pharmacol.* **1984**, *103*, 241–248.
28. Scheffel, U.; Kim, S.; Cline, E. J.; Kuhar, M. J. *Synapse* **1994**, *16*, 263–268.
29. Cline, E. J.; Scheffel, U.; Boja, J. W.; Mitchell, W. M.; Carroll, F. I.; Abraham, P.; Lewin, A. H.; Kuhar, M. J. *Synapse* **1992**, *12*, 37–46.
30. Freed, C.; Revay, R.; Vaughan, R. A.; Kriek, E.; Grant, S.; Uhl, G. R.; Kuhar, M. J. *J. Comp. Neurol.* **1995**, *359*, 340–349.
31. Burchett, S. A.; Bannon, M. J. *Brain Res. Mol. Brain Res.* **1997**, *49*, 95–102.
32. Maggos, C. E.; Spangler, R.; Zhou, Y.; Schlussman, S. D.; Ho, A.; Kreek, M. J. *Synapse* **1997**, *26*, 55–61.